PERGAMON

International Journal of Heat and Mass Transfer 45 (2002) 393–408

International Journal of HEAT and MASS TRANSFER

www.elsevier.com/locate/ijhmt

Natural convection of non-Newtonian fluids through permeable axisymmetric and two-dimensional bodies in a porous medium

Shih-Chieh Wang [a], Cha'o-Kuang Chen [b,*], Yue-Tzu Yang [b]

[a] *Department of Mechanical Engineering, Far East College, Tainan, 744, Taiwan, ROC*

[b] *Department of Mechanical Engineering, National Cheng Kung University, Tainan, 701, Taiwan, ROC*

Received 29 August 2000; received in revised form 23 March 2001

Abstract

The present work concerns the natural convection of non-Newtonian power-law fluids with or without yield stress over the permeable two-dimensional or axisymmetric bodies of arbitrary shape in a fluid-saturated porous medium. Using the fourth-order Runge–Kutta scheme method and shooting method we obtain the local non-similarity solutions. The parameters that include the dimensionless yield stress Ω, permeable constant c and power index n are studied, and the heat flux and the wall temperature are taken into consideration as variables. The local non-similarity solutions are found to be in excellent agreement with the exact solution. It is found that the results depend strongly on the values of the yield stress parameter, the wall temperature distributions, the lateral mass flux rate, and the heat flux at the boundary.

Keywords: Natural convection; Porous medium; Non-Newtonian fluid

1. Introduction

Cheng [1] discussed the Newtonian fluid of natural convection boundary layer on a permeable vertical wall embedded in a saturated porous medium. He found the similarity solutions if the wall temperature and transpiration velocity varied as x^{λ} and $x^{(\lambda-1)/2}$, respectively. Merkin [2] considered the effect of the natural convection of the lateral injection or withdrawal at constant transpiration velocity of Newtonian fluid at constant temperature on a vertical plane wall in a saturated porous medium, as given by Darcy's law.

Liu [3] presented the free convection boundary layer flows of Newtonian fluids on two-dimensional and axisymmetric bodies of arbitrary shape embedded in a saturated porous medium, if the bodies are assumed to be permeable with lateral mass flux and at a constant temperature. He defined a modified stream function to satisfy the same boundary conditions used by Merkin [4] and to get similarity solutions. Nakayama [5] showed that similarity solutions existed for the non-isothermal bodies, which may be either two-dimensional or axisymmetric with arbitrary shapes. Nakayama used the approximate method based on the Karman–Pohlhausen integral relation to get the solutions. Minkowycz [6] used the local non-similarity method to solve Merkin's problem [2]. The results were found to be in good agreement with the finite difference method for the mass flux effects.

Acrivos [7] studied the problem of laminar natural convection heat transfer to non-Newtonian fluids over axisymmetric and two-dimensional bodies of arbitrary shape to show the non-Newtonian effects. Reilly's [8] experimental work was performed for the study of natural convection heat transfer from heated vertical plate to a non-Newtonian fluid and the results agreed with the theoretical analysis of Acrivos's.

The rheological effects of non-Newtonian fluids through porous medium occur in a broad range of

* Corresponding author. Tel.: +886-6-2757575-62140; fax: +886-6-2342081.

E-mail address: ckchen@mail.ncku.edu.tw (C.-K. Chen).

0017-9310/02/$ - see front matter
PII: S0017-9310(01)00123-5

Nomenclature

a	constant, $0 \leqslant a < 1$
b	exponent of Eqs. (26), (32), (47), (52)
c	permeable constant, $-1 \leqslant c \leqslant 1$
E	function of surface temperature, Eq. (23)
f	similarity stream function
g	gravity
G_1	function of shape, Eq. (44)
G_2	function of shape, Eq. (43)
G_3	function of dimensionless temperature, Eq. (44)
h	local heat transfer coefficient of porous medium
H	consistency index
k	permeability
k_{ef}	effective thermal conductivity
ℓ	reference length
m	constant, if $m = 0$ for two-dimensional bodies, if $m = 1$ for three-dimensional axisymmetric bodies
n	power index of non-Newtonian fluids, $n \geqslant 0$
Nu_x	local Nusselt number, Eq. (56)
P	pressure
q^*_w	the surface dimensionless local heat transfer rate, Eq. (55)
q''_w	heat flux of wall surface
Q^*	overall surface dimensionless heat transfer rate, Eq. (59)
Ra_n	modified Rayleigh number, Eq. (9)
R	radial distance
S	variable of shape
T	local temperature of fluid
T_0	reference temperature
u	Darcian velocity in the x direction
v	Darcian velocity in the y direction
$\mathbf{V}$	Darcian velocity vector
W	the width of the two-dimensional body
X	similarity function, Eq. (16)
x, y	coordinates

Greek symbols

α_0	threshold gradient
α_{ef}	effective thermal diffusivity
β	coefficient of thermal expansion
δ_t	dimensionless thermal boundary layer thickness
δ_m	dimensionless momentum boundary layer thickness
$\dot{\gamma}$	shear rate
ϕ	angle
ε	porosity of porous medium
φ	dimensionless stream function, Eqs. (10a) and (10b)
η_1	similarity variable, Eqs. (18a) and (18b)
η_2	similarity variable, Eq. (44)
θ	dimensionless temperature
Ω	dimensionless yield stress, Eq. (9)
ζ	dimensionless variable of body of shape, Eq. (22)
ξ	dimensionless variable
λ	exponent for surface shape
μ	viscosity of Newtonian fluid
μ_{ef}	effective viscosity of non-Newtonian fluid
ρ	density of non-Newtonian fluid
τ	shear stress
τ_0	yield stress
ς	the experimental coefficient
ϕ	angle

Subscripts

0	reference property
ef	effective property
w	wall property
x	local property
∞	ambient property of porous medium

Superscripts

$-$	average property
*	dimensionless property

engineering applications such as transport processes in chemical industry, storage of nuclear waste material and discoveries of the flow of oil in petroleum reservoirs, etc. There are a considerable amount of researches that have been devoted to the study of non-Newtonian power-law fluids in a saturated porous medium with various impermeable surfaces. The researchers are McKinley et al. [9], Pascal [10–12], Chen and Chen [13], Pascal and Pascal [14], Yang and Wang [15] and Getachew et al. [16]. Nevertheless, the former studies [9–16] are restrained to the impermeable surface. The effect of the uniform lateral mass flux in natural convection of non-Newtonian fluids over a cone embedded in a saturated porous medium is solved by Yih [17]; Yih utilizes the implicit finite difference approximation together with the modified Keller box method.

Cheng [18] applied the integral method to obtain the theoretical solution on the combined heat and mass transfer by natural convection from truncated cones in Newtonian fluid-saturated porous medium with variable surface temperature and concentration. Recently, Jumah and Mujumdar [19] investigated the problem of natural convection coupled heat and mass transfer from a vertical flat plate in a porous medium saturated with a Herschel–Bulkley fluid. The major result is that the Lewis number Le and parameter Ω have more significant

effect on the heat and mass transfer rates for a pseudo-plastic fluid compared to the dilatant fluids.

The present work extends the problem of natural convection of flow with or without yield stress over the non-isothermal bodies of arbitrary shape with permeable wall. The governing equations with two different cases of boundary conditions will be discussed, respectively. The first case concerns the performance of both the wall temperature as a power function of distance from the origin and the non-zero lateral mass flux at the boundary under an appropriate distribution. The second case discusses the performance of the flux heating with lateral velocity at the surface of body. In this study, the performance of the wall temperature and constant heat flux are considered. The local non-similarity method was used to solve this problem.

2. Analysis

Owing to non-Newtonian fluids having many rheological behaviors the generalized Bingham rheological model [12] was employed here. The empirical relation can be expressed as

$$\tau = H(\dot{\gamma})^n + \tau_0, \quad \tau > \tau_0, \tag{1}$$

where τ is the shear stress, H is the consistency index, n is the power-law exponent to be determined from experimental test, τ_0 is the yield stress, and $\dot{\gamma}$ is the shear rate. For the values of n which is greater than unity the behavior is dilatant fluid. On the other hand, for the values of n which is less than unity the behavior is pseudo-plastic fluid [20].

The Al-Fariss modified Darcy's law [21], in this study, is used and expressed as:

$$\mathbf{V} = [k(\nabla P - \alpha_0)/\mu_{\mathrm{ef}}]^{1/n}, \tag{2a}$$

which was valid provided that

$$\begin{aligned} &|\nabla P| > \alpha_0; \quad \mathbf{V} \neq \mathbf{0}, \\ &|\nabla P| \leqslant \alpha_0; \quad \mathbf{V} = \mathbf{0}, \end{aligned} \tag{2b}$$

where α_0 was the threshold gradient in the modified Darcy's law and satisfied the following equation:

$$\alpha_0 = \varsigma\tau_0/k^{1/2}, \tag{2c}$$

where ς and k are the experimental coefficient and the permeability of porous medium, respectively. There is the relation of the effective viscosity μ_{ef} as

$$\mu_{\mathrm{ef}} = (1/2)^{(3n+1)/2} H \left(\frac{3n+1}{2}\right)^n (\varepsilon k)^{(1-n)/2} \tag{2d}$$

in which the tortuosity effects have been considered and ε was the porosity of porous medium. When $n = 1.0$, $\alpha_0 = 0$ and $\mu_{\mathrm{ef}} = \mu$ are specified, the Eq. (2a) is a successful approach for a Newtonian fluid with Darcy's law.

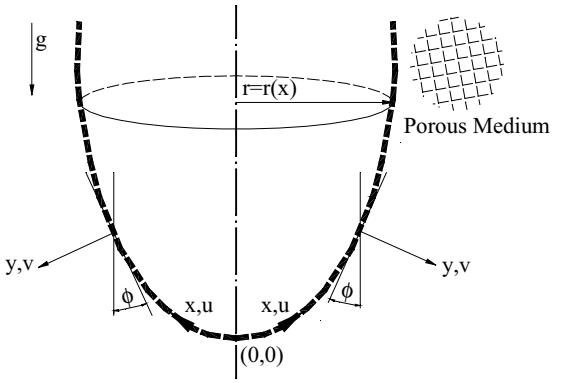

Fig. 1. Physical model and coordinate system.

The physical model and coordinate system in this study are shown in Fig. 1. These governing equations have to obey the following assumptions:

1. Properties of the porous medium and the fluid are constant, unless the density ρ is not constant in the boundary layer.
2. The Boussinesq approximation is employed.
3. The natural convection flow is in uniform steady state and in laminar flow region without turbulence.
4. The viscous dissipation term in the energy equation is neglected, as well as the radiation, chemical reaction, and electromagnetic effects.
5. The convective fluid and the porous medium are in thermodynamic equilibrium at every point in the system, and the temperature of the fluid is below the boiling point. Furthermore, the fluid is not in the neighborhood of the saturation state [22].
6. Without multi-phase zone where mixing of gases, bubbles, vapors, solids and liquids exists in the liquid boundary layer and in the porous medium.

The governing equations with boundary layer simplifications are given as:

1. Equation of continuity:

$$\frac{\partial(r^m u)}{\partial x} + \frac{\partial(r^m v)}{\partial y} = 0, \tag{3}$$

if $m = 0$ for two-dimensional bodies, if $m = 1$ for three-dimensional axisymmetric bodies and $r(x)$ is the radial distance from the axis to surface of the axisymmetric bodies.

2. Momentum equation:

$$u^n = \frac{k\rho_\infty \beta g}{\mu_{\mathrm{ef}}}\left[(T - T_\infty)\cos\phi - \frac{\alpha_0}{\rho_\infty \beta g}\right] \quad \text{if } |(T - T_\infty)\cos\phi| > \frac{\alpha_0}{\rho_\infty \beta g}, \tag{4a}$$

$$u = 0 \quad \text{if } |(T - T_\infty)\cos\phi| \leqslant \frac{\alpha_0}{\rho_\infty \beta g}, \tag{4b}$$

$$\text{where } \cos\phi = [1 - (\mathrm{d}r/\mathrm{d}x)^2]^{1/2}. \tag{4c}$$

3. Energy equation:

$$u\frac{\partial T}{\partial x}+v\frac{\partial T}{\partial y}=\alpha_{\mathrm{ef}}\left(\frac{\partial^2 T}{\partial x^2}+\frac{\partial^2 T}{\partial y^2}\right), \tag{5}$$

where u and v are the modified Darcy's velocities in the x- and y-directions, k is the intrinsic permeability of the porous medium, ρ_∞ is the density of fluid, g is the gravitational acceleration, β is the coefficient of thermal expansion, α_{ef} and μ_{ef} are the effective thermal diffusivity and the effective viscosity of the porous medium saturated with liquid, respectively. When $\phi(x)$ is defined as the angle between the outward tangent and downward vertical of the wall surface Eq. (4c) is satisfied.

In accordance with the boundary layer theory, Eqs. (3)–(5) can be expressed in the following dimensionless form:

$$\frac{\partial (r^*)^m u^*}{\partial x^*}+\frac{\partial (r^*)^m v^*}{\partial y^*}=0, \tag{6}$$

$$\begin{aligned} &u^*=(\theta S-\Omega)^{1/n} \quad \text{if } |\theta S|>\Omega,\\ &u^*=0 \quad \text{if } |\theta S|\leqslant\Omega, \end{aligned} \tag{7}$$

$$u^*\frac{\partial \theta^*}{\partial x^*}+v^*\frac{\partial \theta}{\partial y^*}=\alpha_{\mathrm{ef}}\frac{\partial^2\theta}{\partial y^{*2}}. \tag{8}$$

The dimensionless variables appearing in equations above are defined as

$$\begin{aligned} &r^*=\frac{r}{\ell},\ \ x^*=\frac{x}{\ell},\ \ y^*=\frac{yRa_n^{1/2}}{\ell},\ \theta=\frac{T-T_\infty}{T_0-T_\infty},\\ &S=\cos\phi,\ \ u^*=\frac{u\ell}{Ra_n\alpha_{\mathrm{ef}}},\ \ v^*=\frac{v\ell}{Ra_n^{1/2}\alpha_{\mathrm{ef}}},\\ &\Omega=\frac{\alpha_0}{\rho_\infty\beta g(T_0-T_\infty)} \text{ and } Ra_n=\left[\frac{\rho_\infty\beta g(T_0-T_\infty)}{\mu_{\mathrm{ef}}}\right]^{1/n}\frac{\ell}{\alpha_{\mathrm{ef}}}. \end{aligned} \tag{9}$$

Note that Ra_n is defined as the modified Rayleigh number with n denoting the power-law index; ℓ, T_0 and T_∞ are the reference length, the reference temperature and the temperature outside the boundary layer, respectively. It is suggested that, if T_{w} is a constant then we can set $T_0=T_{\mathrm{w}}$, if T_{w} is not a constant then we can select $T_0=T_{\mathrm{w}}(0)$. In order to satisfy equation of continuity, the dimensionless stream function φ is defined as follows:

$$u^*=\frac{1}{(r^*)^m}\frac{\partial\varphi}{\partial y^*}, \tag{10a}$$

$$v^*=\frac{-1}{(r^*)^m}\frac{\partial\varphi}{\partial x^*}. \tag{10b}$$

Two different cases of the boundary conditions of the Eqs. (6)–(8) are considered that we deal with an important problem. The first case is considered that when surface temperature and the velocity of lateral mass flux are specified. The second case is considered that when surface heat flux and the velocity of lateral mass flux are specified.

2.1. Case 1: The surface temperature and the velocity of lateral mass flux are specified

The surface temperature $T_{\mathrm{w}}(x)$ and the velocity of lateral mass flux $v_{\mathrm{w}}(x)$ are expressed in the following form:

$$v=v_{\mathrm{w}}(x),\ \ T=T_{\mathrm{w}}(x) \quad \text{at } y=0, \tag{11}$$

$$u=0,\ \ T=T_\infty \quad \text{as } y\to\infty. \tag{12}$$

The corresponding dimensionless form can be described as:

$$v^*=v_{\mathrm{w}}^*(x^*),\ \ \theta=\theta_{\mathrm{w}}(x^*) \quad \text{at } y^*=0, \tag{13}$$

$$u^*=0,\ \ \theta=0 \quad \text{as } y^*\to\infty, \tag{14}$$

where

$$v_{\mathrm{w}}^*=\frac{v_{\mathrm{w}}\ell}{Ra_n^{1/2}\alpha_{\mathrm{ef}}},\quad \theta_{\mathrm{w}}=\frac{T_{\mathrm{w}}-T_\infty}{T_0-T_\infty}. \tag{15}$$

The following pseudo-similarity dimensionless transformations are introduced:

$$\begin{aligned} \varphi&=\left\{\int_0^{x^*}(r^*)^{2m}S^{1/n}\,\mathrm{d}\xi\right\}^{1/2}(\theta_{\mathrm{w}}S)^{1/2n}f(\eta_1)\\ &=X(x^*)f(\eta_1), \end{aligned} \tag{16}$$

$$\eta_1=y^*(r^*)^m(\theta_{\mathrm{w}}S)^{1/2n}\left[\int_0^{x^*}(r^*)^{2m}S^{1/n}\,\mathrm{d}\xi\right]^{-1/2}. \tag{17}$$

The dimensionless velocity component in the x- and y-directions can be written as

$$u^*=(\theta_{\mathrm{w}}S)^{1/n}f'(\eta_1), \tag{18a}$$

$$v^*=-\left(X'f(\eta_1)+Xf'\frac{\partial\eta_1}{\partial x^*}\right)/(r^*)^m, \tag{18b}$$

where $f(\eta_1)$ is the similarity dimensionless stream function.

Based on Eqs. (15)–(17), (18a) and (18b), we have

$$\begin{aligned} &\theta_1''+\frac{f\theta_1'}{2}[1+E(\zeta)/n]-E(\zeta)f'\theta_1\\ &\quad=\zeta\left[f'\frac{\partial\theta_1}{\partial\zeta}-\theta_1'\frac{\partial f}{\partial\zeta}\right], \end{aligned} \tag{19}$$

$$f'=\left[\theta_1-\frac{\Omega}{\theta_{\mathrm{w}}S}\right]^{1/n} \quad \text{if } |\theta_1|>|\Omega/(\theta_{\mathrm{w}}S)|, \tag{20a}$$

$$f'=0 \quad \text{if } |\theta_1|\leqslant|\Omega/(\theta_{\mathrm{w}}S)|, \tag{20b}$$

where

$$\theta_1 = \theta/\theta_w, \tag{21}$$

$$\zeta(x^*) = \int_0^{x^*} (r^*)^{2m} S^{1/n}\, d\xi, \tag{22}$$

$$E(\zeta) = \zeta \frac{d \ln \theta_w}{d\zeta}. \tag{23}$$

The boundary conditions for solving Eqs. (19), (20a) and (20b) are

$$f = \frac{-1}{\theta_w^{1/n}\zeta^{1/2}} \int_0^{x^*} (r^*)^m v_w\, d\xi, \quad \theta_1 = 1 \quad \text{at } \eta_1 = 0, \tag{24}$$

$$f' = 0, \quad \theta_1 = 0 \quad \text{as } \eta_1 \to \infty. \tag{25}$$

In order to obtain similarity solutions for Eqs. (19), (20a) and (20b) with boundary conditions, Eqs. (24) and (25), the restrictive interface conditions of following both the conditions 1 and 2 are necessary.

2.1.1. Condition 1

When the surface temperature and the velocity of lateral mass flux are specified the following interface conditions are defined

$$\theta_w = \zeta^b, \quad S = \zeta^{-b}, \quad v_w = c\left(\frac{2b+n}{2n}\right)(r^*)^m \zeta^{1/2}, \tag{26}$$

where $b > (-n/2)$, $c < 0$ for discharge of fluid, $c > 0$ for withdrawal of fluid and the range of c values is $-1 \leqslant c \leqslant 1$. The value of c is called permeable constant, particularly, when $c = 0$ is defined for impermeable surface. The Eqs. (19), (20a), (20b), (24) and (25) can be reduced as:

$$f' = (\theta_1 - \Omega)^{1/n} \quad \text{if } |\theta_1| > \Omega, \tag{27a}$$

$$f' = 0 \quad \text{if } |\theta_1| \leqslant \Omega, \tag{27b}$$

$$\theta_1'' + \left(\frac{n+b}{2n}\right) f\theta_1' - bf'\theta_1 = 0, \tag{28}$$

subject to the boundary conditions

$$f = -c, \quad \theta_1 = 1 \quad \text{at } \eta_1 = 0, \tag{29}$$

$$f' = 0, \quad \theta_1 = 0 \quad \text{as } \eta_1 \to \infty. \tag{30}$$

Note that in the condition 1, if we consider that the body of shape is two-dimensional then we can find the following equation:

$$S = [(b+n)x^*/n]^{-nb/(b+n)}. \tag{31}$$

2.1.2. Condition 2

The interface conditions are defined as

$$\theta_w = \zeta^b, \quad \Omega = 0,$$
$$v_w = c\left(\frac{2b+n}{2n}\right)(r^*)^m S^{1/n} \zeta^{(2b+n)/2n}, \tag{32}$$

where b and c are constants; the value of c is $-1 \leqslant c \leqslant 1$; the value of b is an arbitrary real number which is greater than or equal to zero. Eq. (32) is for the fluid without yield stress through arbitrary three-dimensional axisymmetric or two-dimensional bodies with permeable surface in a porous medium. Substituting Eq. (32) into Eqs. (19), (20a), (20b), (24) and (25), yields the following dimensionless ordinary differential governing equations:

$$f' = \theta_1^{1/n}, \tag{33}$$

$$\theta_1'' + \left(\frac{n+b}{2n}\right) f\theta_1' - bf'\theta_1 = 0, \tag{34}$$

subject to the boundary conditions

$$f = -c, \quad \theta_1 = 1 \quad \text{at } \eta_1 = 0, \tag{35}$$

$$f' = 0, \quad \theta_1 = 0 \quad \text{as } \eta_1 \to \infty. \tag{36}$$

2.2. Case 2: The surface heat flux and the velocity of lateral mass flux are specified

Let the value of heat flux q_w'' not be a constant and the value of velocity $v_w(x)$ of lateral mass flux on surface not be zero. When above conditions are taken into consideration the boundary conditions for solving Eqs. (3)–(5) are described as:

$$v = v_w(x), \quad \frac{\partial T}{\partial y} = -\frac{q_w''(x)}{k_{ef}} \quad \text{at } y = 0, \tag{37}$$

$$u = 0, \quad T = T_\infty \quad \text{as } y \to \infty. \tag{38}$$

Introducing new dimensionless variables, Eqs. (11) and (12) can be written as

$$v^* = v_w^*(x^*), \quad \frac{\partial \theta}{\partial y^*} = -\theta_r(x^*) \quad \text{at } y^* = 0, \tag{39}$$

$$u^* = 0, \quad \theta = 0 \quad \text{as } y^* \to \infty, \tag{40}$$

where

$$\theta_r = \frac{q_w''(x)\ell}{k_{ef}(T_0 - T_\infty)Ra_n^{1/2}} = -\frac{\partial \theta}{\partial y^*}\Big|_{y^*=0}. \tag{41}$$

A new variable θ_2 is introduced for this case

$$\theta_2 = \frac{S^{1/(2n+1)}}{[x^*\theta_r^2]^{n/(2n+1)}}\theta. \tag{42}$$

The following general dimensionless variables are presented as

$$\varphi = \left[(x^*)^{(n+1)}\theta_r S\right]^{1/(2n+1)} (r^*)^m f(\eta_2), \tag{43}$$

$$\eta_2 = y^*[\theta_r S (x^*)^{-n}]^{1/(2n+1)}. \tag{44}$$

The dimensionless velocity component in the x direction will be written as

$$u^* = (\theta_r^2 S^2 x^*)^{1/(2n+1)} f'(\eta_2). \tag{45}$$

Accordingly, based on Eqs. (7), (8), (13) and (14), the following equations can be obtained

$$f' = \left[\theta_2 - \Omega/(x^*\theta_r^2 S^2)^{n/(2n+1)}\right]^{1/n}$$
$$\text{if } |\theta_2| > \left|\Omega/(x^*\theta_r^2 S^2)^{n/(2n+1)}\right|, \tag{46a}$$

$$f' = 0 \quad \text{if } |\theta_2| \leqslant \left|\Omega/(x^*\theta_r^2 S^2)^{n/(2n+1)}\right|, \tag{46b}$$

$$\theta_2'' + \frac{f\theta_2'}{2}\left[\frac{n+1}{2n+1} + \frac{G_1+G_3}{2n+1} + G_2\right] - \frac{n}{2n+1} \times \left[1 + 2G_3 - \frac{G_1}{n}\right] f'\theta_2 = x^*\left[f'\frac{\partial\theta_2}{\partial x^*} - \theta_2'\frac{\partial f}{\partial x^*}\right], \tag{47}$$

where

$$G_1(x^*) = x^*\frac{\mathrm{d}\ln S}{\mathrm{d}x^*}, \tag{48}$$

$$G_2(x^*) = x^*\frac{\mathrm{d}\ln (r^*)^m}{\mathrm{d}x^*}, \tag{49}$$

$$G_3(x^*) = x^*\frac{\mathrm{d}\ln \theta_r}{\mathrm{d}x^*}. \tag{50}$$

The boundary conditions for solving Eqs. (19), (20a) and (20b) are

$$f = \frac{-1}{(r^*)^m[(x^*)^{(n+1)}\theta_r S]^{1/(2n+1)}}\int_0^{x^*}(r^*)^m v_{\mathrm{w}}\,\mathrm{d}\xi,$$
$$\theta_2' = -1 \quad \text{at } \eta_2 = 0, \tag{51}$$

$$f' = 0,\ \ \theta_2 = 0 \quad \text{as } \eta_2 \to \infty. \tag{52}$$

In order to get local non-similarity solutions in this case, the restrictive interface conditions of following both the conditions 3 and 4 are necessary.

2.2.1. Condition 3

It is defined as the non-Newtonian fluids with yield stress through some two-dimensional bodies (i.e., $m = 0$) in a porous medium and the interface conditions are considered as

$$\theta_r = (x^*)^b, \quad S = (x^*)^{-b-0.5}, \quad v_{\mathrm{w}} = -0.5c(x^*)^{-1.5}, \tag{53}$$

where $-1 \leqslant c \leqslant 1$, the value of b is an arbitrary real number. In accordance with the Eq. (53), these Eqs. (46a), (46b), (47), (51) and (52) can be reduced as:

$$f' = (\theta_2 - \Omega)^{1/n} \quad \text{if } |\theta_2| > \Omega, \tag{54a}$$
$$f' = 0 \quad \text{if } |\theta_2| \leqslant \Omega, \tag{54b}$$

$$\theta_2'' + 0.5f\theta_2' - (b+0.5)f'\theta_2 = 0, \tag{55}$$

subject to the boundary conditions

$$f = -c,\ \ \theta_2' = -1 \quad \text{at } \eta_2 = 0, \tag{56}$$

$$f' = 0,\ \ \theta_2 = 0 \quad \text{as } \eta_2 \to \infty. \tag{57}$$

2.2.2. Condition 4

It is defined as the non-Newtonian fluids without yield stress through some three-dimensional axisymmetric or two-dimensional bodies and is conformed to the following interface conditions

$$v_{\mathrm{w}} = c(x^*)^{(2mn+m+n+b-n)/(2n+1)}a^{1/(2n+1)}(1-a^2)^{m/2} \times \left[\frac{2mn+m+n+b+1}{2n+1}\right], \quad b+m+1 \neq 0, \tag{58}$$

where a and c are constants; the values of a and c are $0 \leqslant a < 1$ and $-1 \leqslant c \leqslant 1$, respectively. Here we can obtain the function of r^*, that is $r^* = (1-a^2)^{1/2}x^*$. Using Eq. (58), the Eqs. (46a), (46b), (47), (51) and (52) could be transformed as:

$$f' = \theta_2^{1/n}, \tag{59}$$

$$\theta_2'' + \left(1 + \frac{n+b+1}{2n+1}\right)f\theta_2' - \frac{n(2b+1)}{2n+1}f'\theta_2 = 0. \tag{60}$$

The boundary conditions are the same as Eqs. (56) and (57).

2.3. Heat transfer rate and Nusselt number

According to Fourier's law of conduction, the surface dimensionless local heat transfer rate $q_{\mathrm{w}}^*(x)$ can be written as:

$$q_{\mathrm{w}}^*(x) = \frac{q_{\mathrm{w}}''(x)\ell}{(T_0 - T_\infty)k_{\mathrm{ef}}} = \frac{-\ell}{(T_0 - T_\infty)}\frac{\partial T}{\partial y}\Big|_{y=0} = -Ra_n^{1/2}\frac{\partial\theta}{\partial y^*}\Big|_{y^*=0}. \tag{61}$$

The local Nusselt number Nu_x can be expressed as

$$Nu_x = \frac{hx}{k_{\mathrm{ef}}} = \frac{q_{\mathrm{w}}''(x)x}{k_{\mathrm{ef}}(T_{\mathrm{w}} - T_\infty)} = \frac{-x^*Ra_n^{1/2}}{\theta_{\mathrm{w}}}\frac{\partial\theta}{\partial y^*}\Big|_{y^*=0}, \tag{62}$$

where h denotes the local heat transfer coefficient of the non-Newtonian fluid in a fluid-saturated porous medium.

The average heat transfer coefficient $\bar{h}$ can be expressed as

$$\bar{h} = \frac{1}{\ell}\int_0^\ell h\,\mathrm{d}x = -\frac{k_{\mathrm{ef}}Ra_n^{1/2}}{\ell}\int_0^1 \theta_{\mathrm{w}}\frac{\partial\theta}{\partial y^*}\Big|_{y^*=0}\mathrm{d}x^*. \tag{63}$$

The average Nusselt number $\overline{Nu}$ can be written as

$$\overline{Nu} = \frac{\bar{h}\ell}{k_{\mathrm{ef}}} = -Ra_n^{1/2}\int_0^1 \theta_{\mathrm{w}}\frac{\partial\theta}{\partial y^*}\Big|_{y^*=0}\mathrm{d}x^*. \tag{64}$$

The overall surface dimensionless heat transfer rate can be calculated by the following equation:

$$Q^* = \frac{\int_0^\ell (2\pi r)^m (2W)^{(1-m)} q''_w(x)\mathrm{d}x}{k_{ef}(T_0 - T_\infty)/\ell} = -2\pi^m Ra_n^{1/2} \int_0^1 (r^*)^m (W^*)^{(1-m)} \frac{\partial\theta}{\partial y^*}\Big|_{y^*=0} \mathrm{d}x^*, \quad (65)$$

where W is the width of the two-dimensional body and $W^* = W/\ell$. The overall surface heat transfer rate can be calculated by $Q = Q^* k_{ef}(T_0 - T_\infty)/\ell$.

3. Results and discussion

3.1. Exact solutions

It is showed that exact solutions to Eqs. (33)–(36) exist if the constant b is equal to the power index n in condition 2. Under such a restricted condition, we can get exact solutions as:

$$\theta_1 = \exp\{-[(c^2+4n)^{1/2} - c]\eta_1/2\}, \quad (66a)$$

$$f = \frac{-2n}{(c^2+4n)^{1/2} - c}\left[\exp^{-\left(\frac{(c^2+4n)^{1/2}-c}{2n}\eta_1\right)} - 1\right] - c, \quad n > 0. \quad (66b)$$

Fig. 2 shows the effects of the power index n and permeable constant c on the dimensionless temperature θ_1 and similarity stream function f profiles. The dimensionless temperature distributions are considered when $c = 0.0$, $n = 1.0$, $b = 1.0$ and $c = 1.0$, $n = 2.0$, $b = 2.0$. The different distribution profiles are found obviously when $c = 1.0$, $n = 0.1$ and $b = 0.1$. The expressions for the dimensionless thermal (δ_t) and momentum (δ_m) boundary layer thickness can be obtained from Eqs. (66a) and (66b) if the edges of the boundary layers are defined as the points where $\theta/\theta_w = \theta_1$ or $[f'(\eta)/f'(0)]$ has a value of 0.01. The dimensionless thermal and momentum boundary layer thickness then can be expressed exactly as

$$\delta_t = 4\ln(10)/[(c^2+4n)^{1/2} - c],$$
$$\delta_m = 4n\ln(10)/[(c^2+4n)^{1/2} - c].$$

In addition, the interesting relation $\delta_m/\delta_t = n$ is found by considering the above conditions. It can be seen from Fig. 3 that δ_t increases as n decreases and δ_m increases with n when c is fixed. As illustrated in Fig. 3, the values of δ_t are smaller than 10.0 if the power index $n > 0.7$, and the values of δ_m are smaller than 10.0 if $n < 2.5$. When we solve the problems numerically, both the values of $\theta_1'(0)$ and the values of η_∞ for $f'(\eta_\infty) = 0$ which are good for predicting the value of temperature gradient on the surface and how large is the value of similarity variable η_∞ is enough. As an example, if we want to obtain solutions, under the conditions $c = 1$, $n = 0.1$ and $b = 0.1$ then we have to set $\eta_\infty > 50.27$ and $\theta_1'(0) = 0.0916078$ for initial conditions of numerical solutions.

For condition 4, if the constant b is equal to $(3n+1)$ and the constant c is equal to zero, the exact solutions of Eqs. (59) and (60) are expressed as:

$$\theta_2 = \frac{\exp[-(3n)^{n/(2n+1)}\eta_2]}{(3n)^{n/(2n+1)}}, \quad (67a)$$

$$f = \frac{n[1 - \exp(-(3n)^{n/(2n+1)}\eta_2/n)]}{(3n)^{(n+1)/(2n+1)}}. \quad (67b)$$

Under above Eqs. (67a) and (67b), the dimensionless thermal and momentum boundary layer thicknesses also can be expressed correctly as $\delta_t = 2\ln(10)/(3n)^{n/(2n+1)}$ and $\delta_m = 2n\ln(10)/(3n)^{n/(2n+1)}$, respectively. It is seen

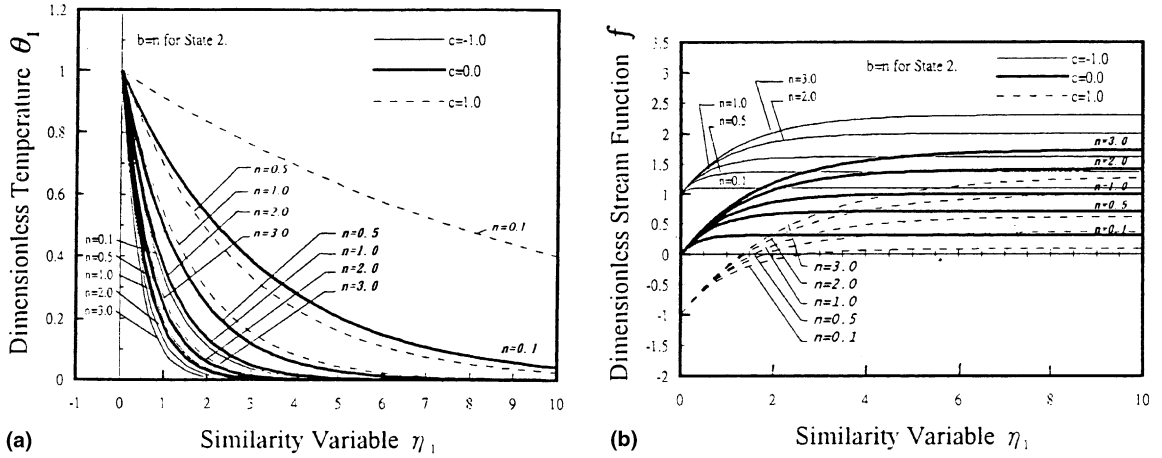

Fig. 2. The dimensionless temperature and similarity stream function profiles versus η_1 for various values of power index n and permeable constant c in the condition 2.

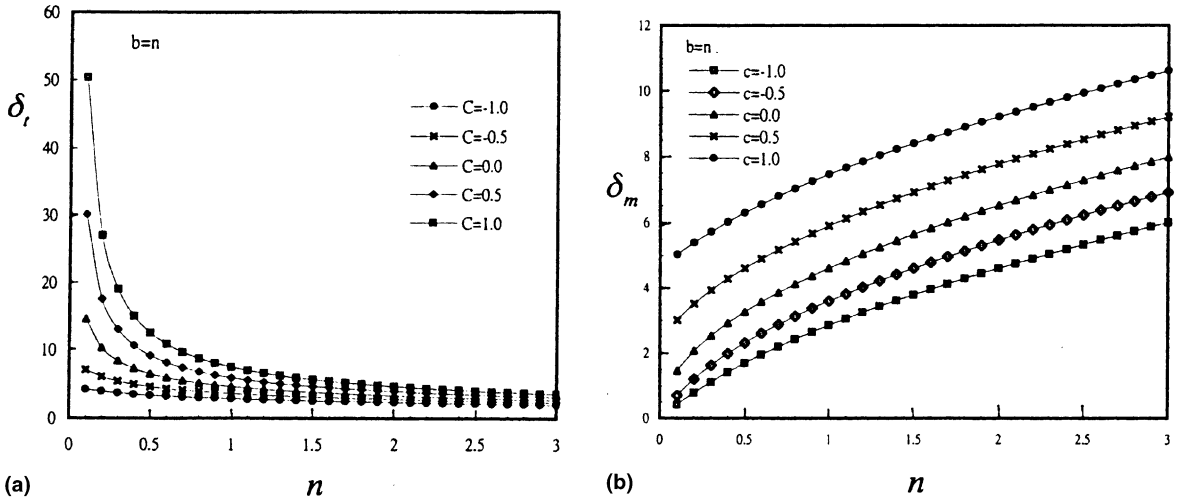

Fig. 3. The dimensionless thermal (δ_t) and momentum (δ_m) boundary layer thickness versus power index n in the condition 2.

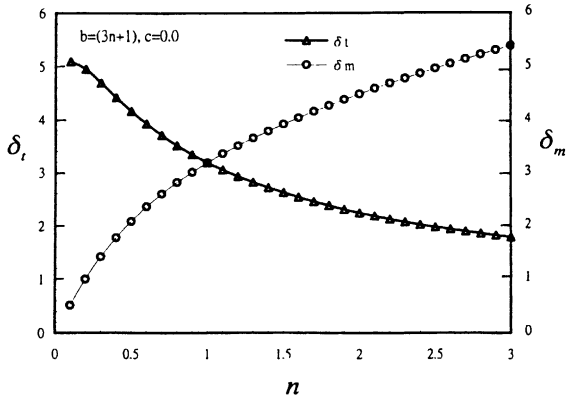

Fig. 4. The dimensionless thermal (δ_t) and momentum (δ_m) boundary layer thickness versus power index n in the condition 4.

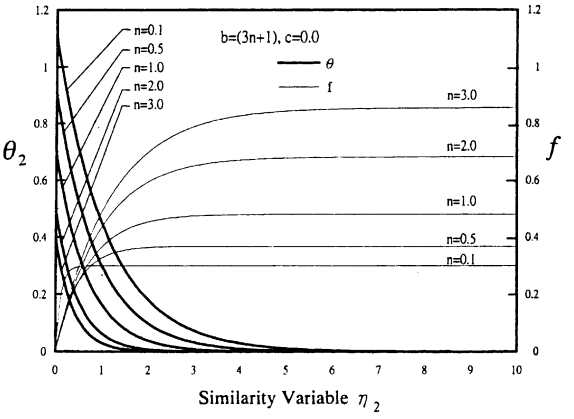

Fig. 5. The dimensionless temperature θ and similarity stream function f profiles versus η_2 for various values of power index n for $c = 0$ in the condition 4.

from Fig. 4 that δ_t increases as n decreases and δ_m increases with n. Simultaneously, we are able to find $\delta_t = \delta_m$ if the power index n is equal to unity. Fig. 5 shows the effects of the power index n on the dimensionless temperature and similarity stream function distributions for impermeable surface. It is seen from Fig. 5 that $f(\infty)$ increases with n and $\theta(0)$ decreases as n increases when the value of c is equal to zero and b is equal to $(3n+1)$. Using the definition

$$b = (3n+1) \text{ and}$$
$$c = n(3n)^{-(n+1)/(2n+1)} - (3n)^{n/(2n+1)}/3 \tag{68}$$

the exact solutions of dimensionless temperature θ_2 and similarity stream function f in condition 4 can be expressed as the following equation:

$$\theta_2 = \frac{\exp\left[-(3n)^{n/(2n+1)}\eta_2\right]}{(3n)^{n/(2n+1)}}, \tag{69a}$$

$$f = \frac{n[1-\exp(-(3n)^{n/(2n+1)}\eta_2/n)]}{(3n)^{(n+1)/(2n+1)}} - c. \tag{69b}$$

We have to assume the initial value of $\theta_2(0)$ and η_∞, when the shooting method is used to solve the problem numerically. The above results can be utilized to reinforce the accuracy of initial value.

3.2. The local non-similarity solutions

In this study, local non-similarity solutions are obtained by using the fourth-order Runge–Kutta scheme and the shooting method. Let us consider the results. There are four conditions to examine.

3.2.1. Condition 1

For the condition 1, the step-sizes $\Delta\eta = 0.001$ and the value $\eta_\infty = 20.0$ were employed. On the other hand, we have to use $\Delta\eta < 0.001$ and $\eta_\infty > 20.0$ if $n < 0.2$ or $\Omega > 0.3$. The values of $[-\theta_1'(0)]$ for various values of power index n, the permeable constant c, and the yield stress parameter Ω are shown in Table 1. In Table 1, if the parameters c and n are fixed then the dimensionless temperature gradient on surface $[-\theta_1'(0)]$ increases with Ω. Also, the values of $[-\theta_1'(0)]$ decrease as the value of c increases when the values of n and Ω are fixed.

The power index n and the permeable constant c effects are presented in Figs. 6 and 7, which show the dimensionless temperature profiles and the dimensionless stream function profiles.

The power index n effects: Fig. 6 shows that both the dimensionless thermal boundary layer thickness δ_t and the dimensionless momentum boundary layer thickness δ_m increase with n if the parameters b, c, and Ω are fixed. Besides, the values of $f(\infty)$ increase with power index n if the values of b, c and Ω are fixed.

Table 1
Value of $[-\theta_1'(0)]$ when $b = 0.5$ for condition 1 for the selected power index values of n

$-\theta_1'(0)$	$\Omega = 0.1$			$\Omega = 0.3$		
	$c = 0.0$	$c = 1.0$	$c = -1.0$	$c = 0.0$	$c = 1.0$	$c = -1.0$
$n = 0.25$	0.495623	0.174742	1.643762	0.270265	0.069117	1.542840
$n = 0.5$	0.610144	0.298646	1.284695	0.427352	0.184384	1.149843
$n = 1.0$	0.705021	0.416326	1.176628	0.565566	0.317962	1.046213
$n = 2.0$	0.774323	0.504118	1.158620	0.668687	0.428384	1.047499
$n = 3.0$	0.803006	0.540152	1.160721	0.711981	0.475908	1.060492

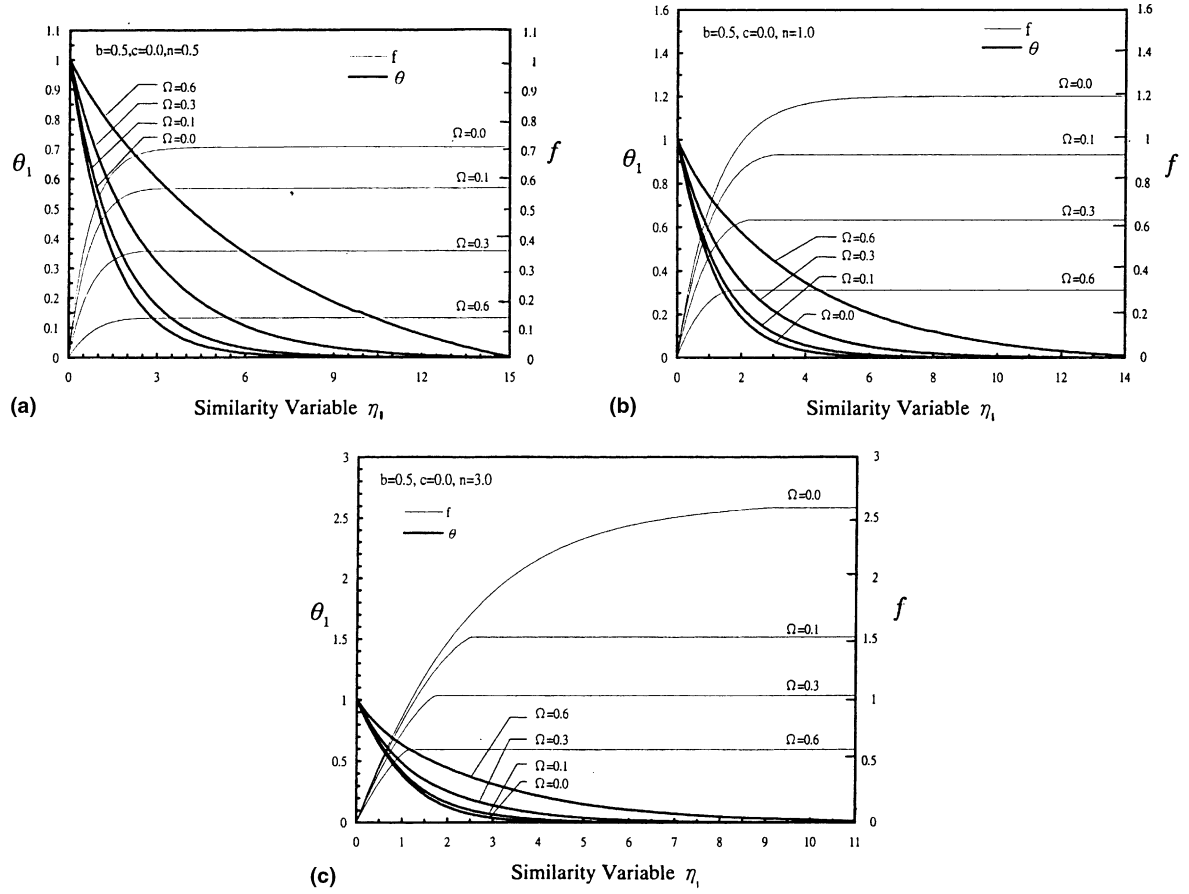

Fig. 6. The dimensionless temperature and similarity stream function profiles versus η_1 for various values of dimensionless yield stress Ω when $b = 0.5$, $c = 0.0$ in the condition 1.

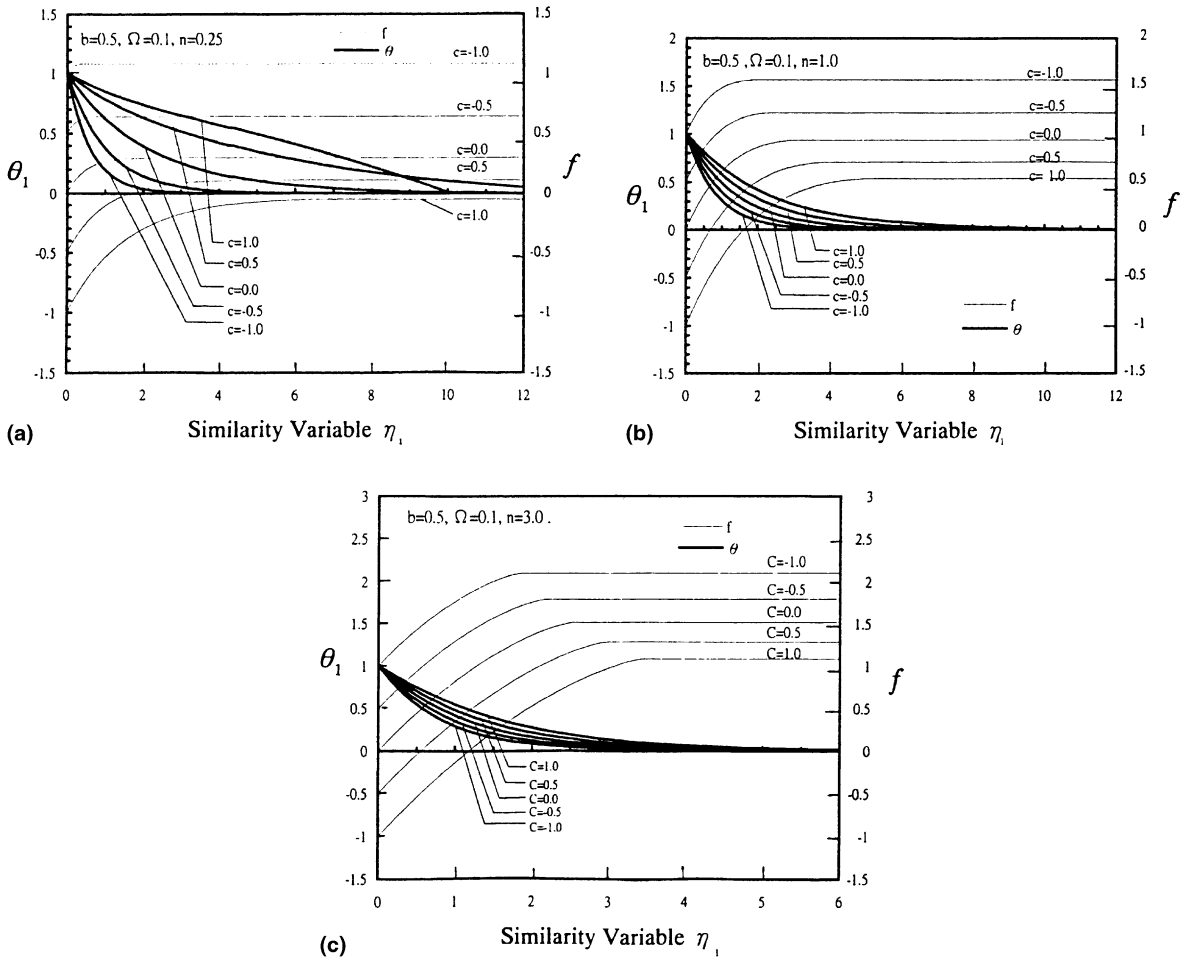

Fig. 7. The dimensionless temperature and similarity stream function profiles versus η_1 for various values of permeable constant c when $b = 0.5$, $\Omega = 0.1$ in the condition 1.

The yield stress parameter Ω effects: It is seen from Fig. 6 that the dimensionless thermal boundary layer thickness δ_t increases with Ω and the dimensionless momentum boundary layer thickness δ_m decreases as Ω increases if the parameters b, c, and n are fixed. Especially, the effect of power index Ω for δ_m of dilatent fluids ($n = 3$) is more evident than the others ($n < 3$).

The permeable constant c effects: It is found from Fig. 7 that both the dimensionless thermal boundary layer thickness δ_t and the dimensionless momentum boundary layer thickness δ_m increase with c if the parameters b, Ω, and n are fixed. The effect of permeable constant c for the dimensionless temperature profiles of pseudoplastic fluids ($n = 0.25$) can be seen from Fig. 7(a) that it is very different from the other fluids. In condition 1, it is found that Eqs. (61)–(65) can be rewritten as:

$$q_w^*(x^*) = -\theta_1'(0) Ra_n^{1/2} (r^*)^m \zeta^{(2b-1)/2}, \tag{70}$$

$$Nu_x = -\theta_1'(0) x^* Ra_n^{1/2} (r^*)^m \zeta^{-1/2}, \tag{71}$$

$$\overline{Nu} = -\theta_1'(0) Ra_n^{1/2} \int_0^1 (r^*)^m \zeta^{-0.5} \, dx^* \tag{73}$$

$$Q^* = -2\pi^m (W^*)^{1-m} \theta_1'(0) Ra_n^{1/2} \int_0^1 (r^*)^{2m} \zeta^{(2b-1)/2} \, dx^*. \tag{74}$$

3.2.2. Condition 2

For the condition 2, the step-sizes $\Delta\eta = 0.0001$ and the value $\eta_\infty = 20.0$ were employed. The numerical values of $[-\theta_1'(0)]$ for various values of power index n and the permeable constant c are shown in Table 2. The results are seen to be in good agreement with the exact solutions within 0.0253% discrepancy.

The power index n effects: It can be seen from Fig. 8 that the trend of the profiles of the dimensionless stream function f is a straight line for $n < 0.5$. From Fig. 8, it is quite obvious that there is not much alteration in the profiles of the dimensionless temperature for $c = 1.0$

Table 2
Compare value of $[-\theta_1'(0)]$ of numerical solutions and exact solutions when $b = n$ for condition 2

$-\theta_1'(0)$	$c = 0.0$		$c = 1.0$		$c = -1.0$	
	Numerical	Exact	Numerical	Exact	Numerical	Exact
$n = 0.25$	0.500001	0.500000	0.2071087	0.2071068	1.207130	1.207107
$n = 0.5$	0.707183	0.707106	0.3661597	0.3660254	1.365680	1.366025
$n = 0.75$	0.866026	0.866025	0.5000010	0.5000000	1.500006	1.500000
$n = 1.00$	1.000000	1.000000	0.6180364	0.6180340	1.618047	1.618034
$n = 1.5$	1.224745	1.224745	0.8228779	0.8228756	1.822912	1.822876
$n = 2.0$	1.414213	1.414214	1.0000027	1.0000000	2.000062	2.000000
$n = 3.0$	1.732063	1.732051	1.3027680	1.3027760	2.302693	2.302776

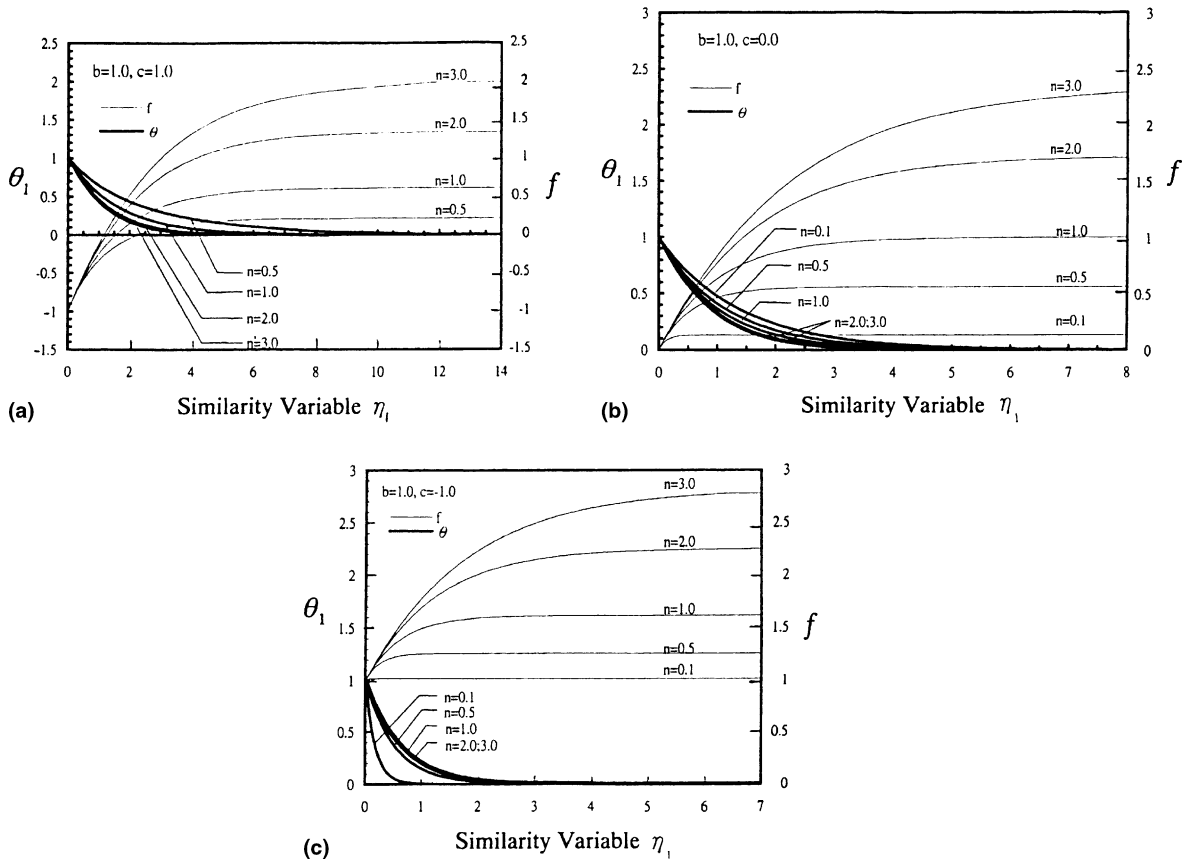

Fig. 8. The dimensionless temperature and similarity stream function profiles versus η_1 for various values of power index n when $b = 1.0$ in the condition 2.

(withdrawal of fluid). In condition 2, it is found that Eqs. (61)–(65) can be rewritten as:

$$q_w^*(x^*) = -\theta_1'(0) Ra_n^{1/2} (r^*)^m S^{1/2n} \zeta^{(b-n+2nb)/2n}, \tag{75}$$

$$Nu_x = -\theta_1'(0) x^* Ra_n^{1/2} (r^*)^m S^{1/2n} \zeta^{(b-n)/2n}, \tag{76}$$

$$\overline{h} = -\frac{k_{ef}}{\ell} \theta_1'(0) Ra_n^{1/2} \int_0^1 (r^*)^m S^{1/2n} \zeta^{(b-n)/2n} \, dx^*, \tag{77}$$

$$\overline{Nu} = -\theta_1'(0) Ra_n^{1/2} \int_0^1 (r^*)^m S^{1/2n} \zeta^{(b-n)/2n} \, dx^*, \tag{78}$$

$$Q^* = -2\pi^m (W^*)^{(1-m)} \theta_1'(0) Ra_n^{1/2} \times \int_0^1 (r^*)^{2m} S^{1/2n} \zeta^{(b-n+2nb)/2n} \, dx^*. \tag{79}$$

3.2.3. Condition 3

For the condition 3, the step-sizes $\Delta\eta = 0.001$ and the value $\eta_\infty = 30.0$ were employed. The numerical values of $\theta_2(0)$ for various values of power index n, the permeable constant c, and the yield stress parameter Ω are shown in

Table 3. It can be seen from Fig. 9 that the values of $\theta_2(0)$ and the dimensionless thermal boundary layer thickness δ_t increase with Ω for $-1 \leqslant c \leqslant 1$. In regard to the value of $f(\infty)$, we can find that it decreases as the value of c increases. From Fig. 9, it is very clear that there is not much alteration in the values of the dimensionless temperature on the wall surface $\theta_2(0)$ when b, Ω, and $0 \leqslant c \leqslant 1$ are fixed. But the values of $\theta_2(0)$ have much alteration for discharging effects $-1 \leqslant c < 0$, as shown in Fig. 10. The Eqs. (61)–(65) can be rewritten as:

$$q_w^*(x^*) = Ra_n^{1/2}(x^*)^b, \tag{80}$$

$$Nu_x = Ra_n^{1/2}(x^*)^{(n+0.5)/(2n+1)}/\theta_2(0), \tag{81}$$

$$\overline{h} = 2Ra_n^{1/2}k_{ef}/[\theta_2(0)\ell], \tag{82}$$

$$\overline{Nu} = 2Ra_n^{1/2}/\theta_2(0), \tag{83}$$

Table 3
Value of $\theta_2(0)$ when $b = 0.5$ for condition 3 for the selected power index values of n

$\theta_2(0)$	$\Omega = 0.1$			$\Omega = 0.3$		
	$c = 0.0$	$c = 1.0$	$c = -1.0$	$c = 0.0$	$c = 1.0$	$c = -1.0$
$n = 0.1$	1.237487	1.2596157	1.175618	1.422377	1.444833	1.343474
$n = 0.5$	1.203991	1.3217958	1.040076	1.350715	1.468962	1.164503
$n = 1.0$	1.123101	1.2939429	0.937183	1.245441	1.414543	1.044229
$n = 2.0$	1.041077	1.2481310	0.850165	1.140304	1.341392	0.942338
$n = 3.0$	1.002440	1.222219	0.812374	1.090592	1.301566	0.897609

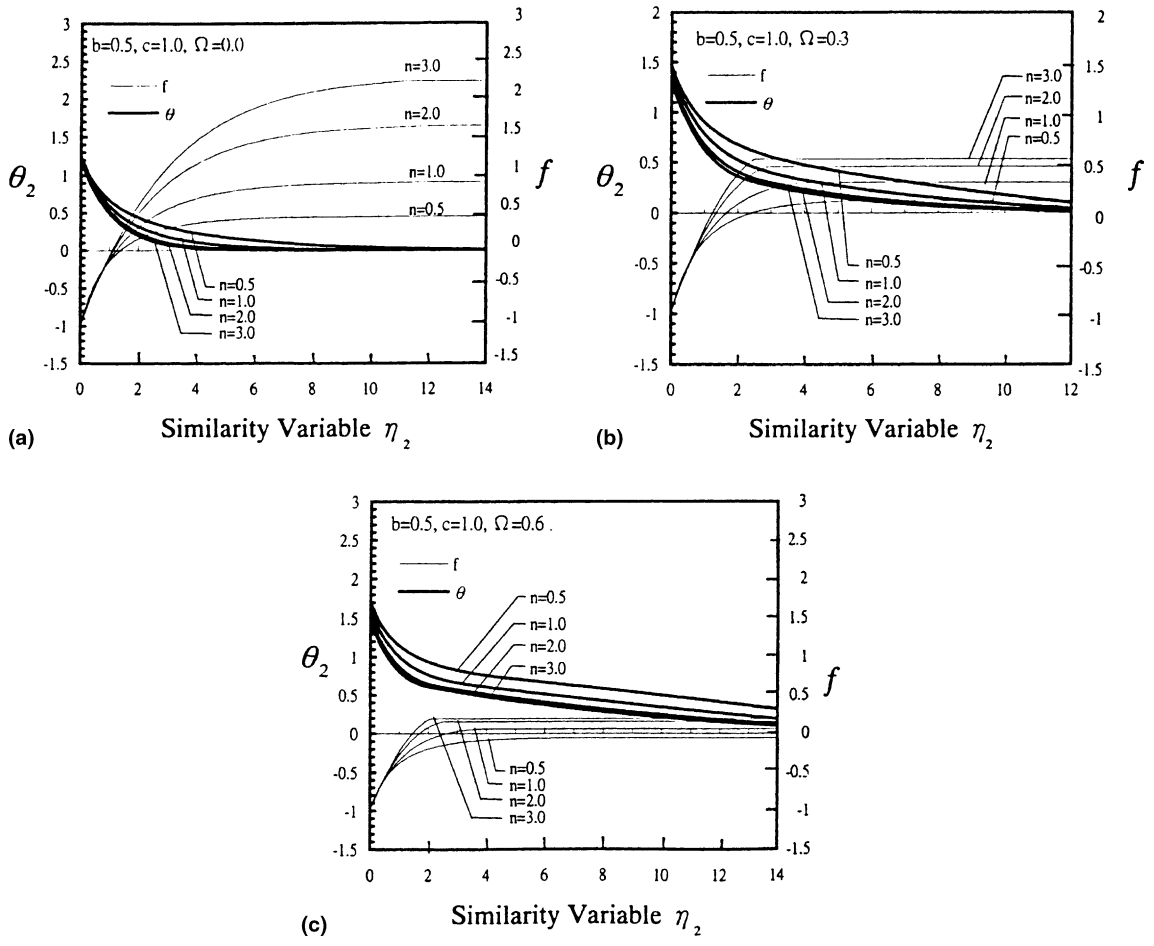

Fig. 9. The dimensionless temperature and similarity stream function profiles versus η_2 for various values of power index n when $b = 0.5$, $c = 1.0$ in the condition 3.

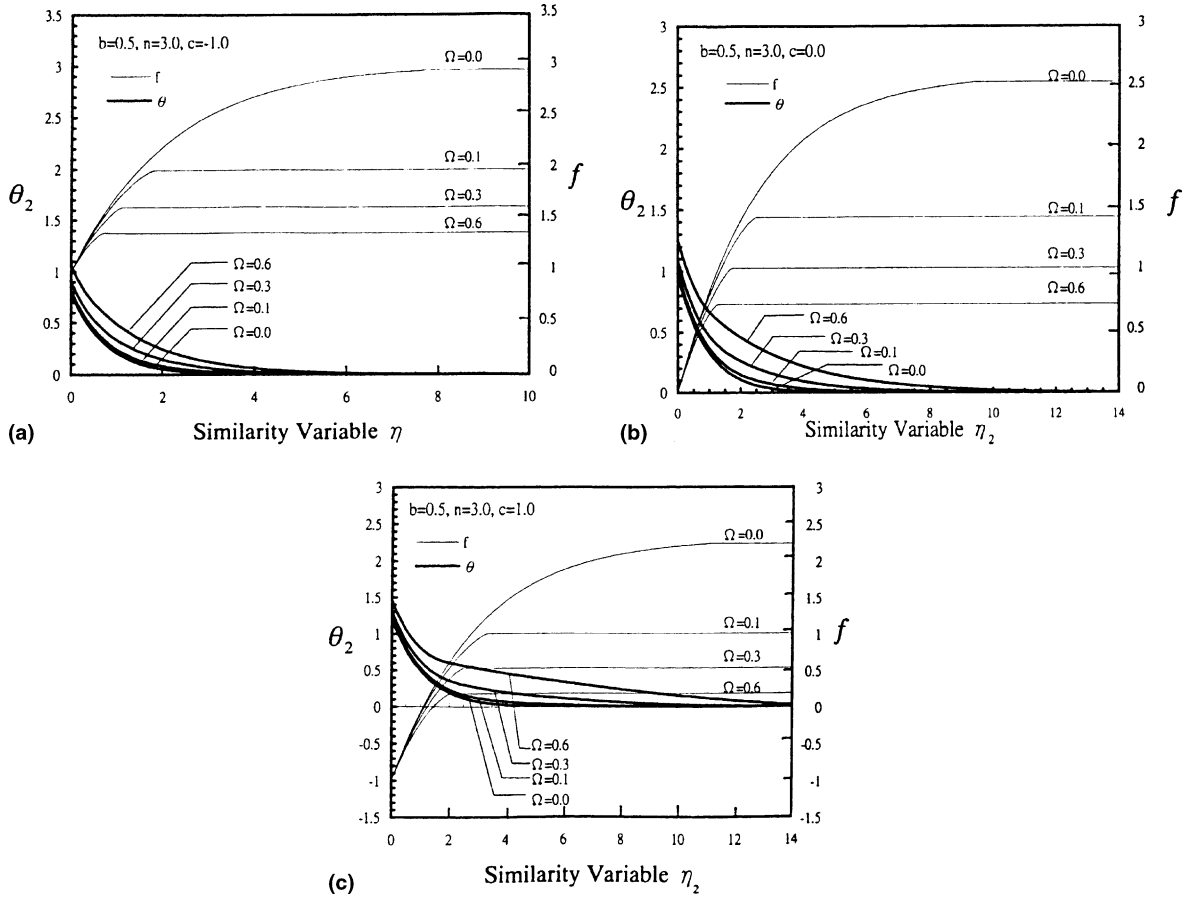

Fig. 10. The dimensionless temperature and similarity stream function profiles versus η_2 for various values of dimensionless yield stress Ω when $b = 0.5$, $n = 3.0$ in the condition 3.

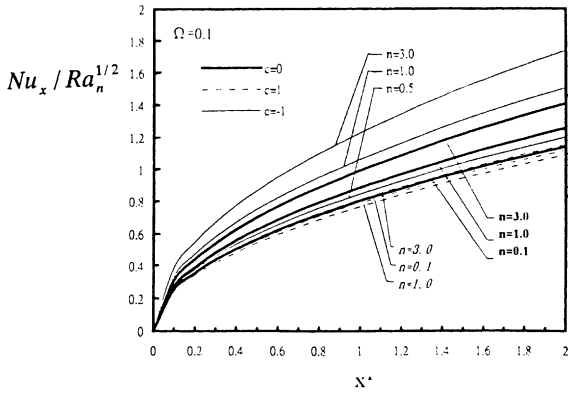

Fig. 11. The values of $Nu_x/Ra_n^{1/2}$ versus x^* for various values of power index n and permeable constant c in the condition 3.

$$Q^* = 2Ra_n^{1/2}W^*/(b+1) \quad \text{for } b > -1. \tag{84}$$

If we consider the surface shape to be a vertical plane then we have to select the exact value of b which is equal to $(-1/2)$. The values of the local Nusselt number $Nu_x/Ra_n^{1/2}$ increase with the power index n and decrease as the value of c increases except $c = 1$ as shown Fig. 11.

3.2.4. Condition 4

For the condition 4, the step-sizes $\Delta\eta = 0.001$ and the value $\eta_\infty = 15.0$ were employed. The numerical values of $[\theta_2(0)]$ for various values of power index n and the permeable constant c are shown in Table 4. It can be seen that there is agreement by comparing with the exact results. The maximum error is under 0.157%.

The permeable constant c effects: From Fig. 12, it can be seen that the values of $\theta_2(0)$, the dimensionless momentum boundary layer thickness δ_m and the dimensionless thermal boundary layer thickness δ_t increase with c when the values of b and n are fixed. Moreover, the value of $f(\infty)$ decreases as the value of c increases and the trend of it is still equal if $c > 0$. These Eqs. (61)–(65) can be rewritten as:

Table 4
Compare value of $\theta_2(0)$ of numerical solutions and exact solutions when $b = 3n + 1$ for condition 4

$\theta_2(0)$	$n = 0.1$	$n = 0.5$	$n = 1.0$	$n = 2.0$	$n = 3.0$
Numerical	1.1046523	0.9032978	0.6930148	0.4878512	0.389365
Exact	1.105537	0.903602	0.693361	0.488359	0.389977
Error (%)	0.080	0.034	0.050	0.104	0.157

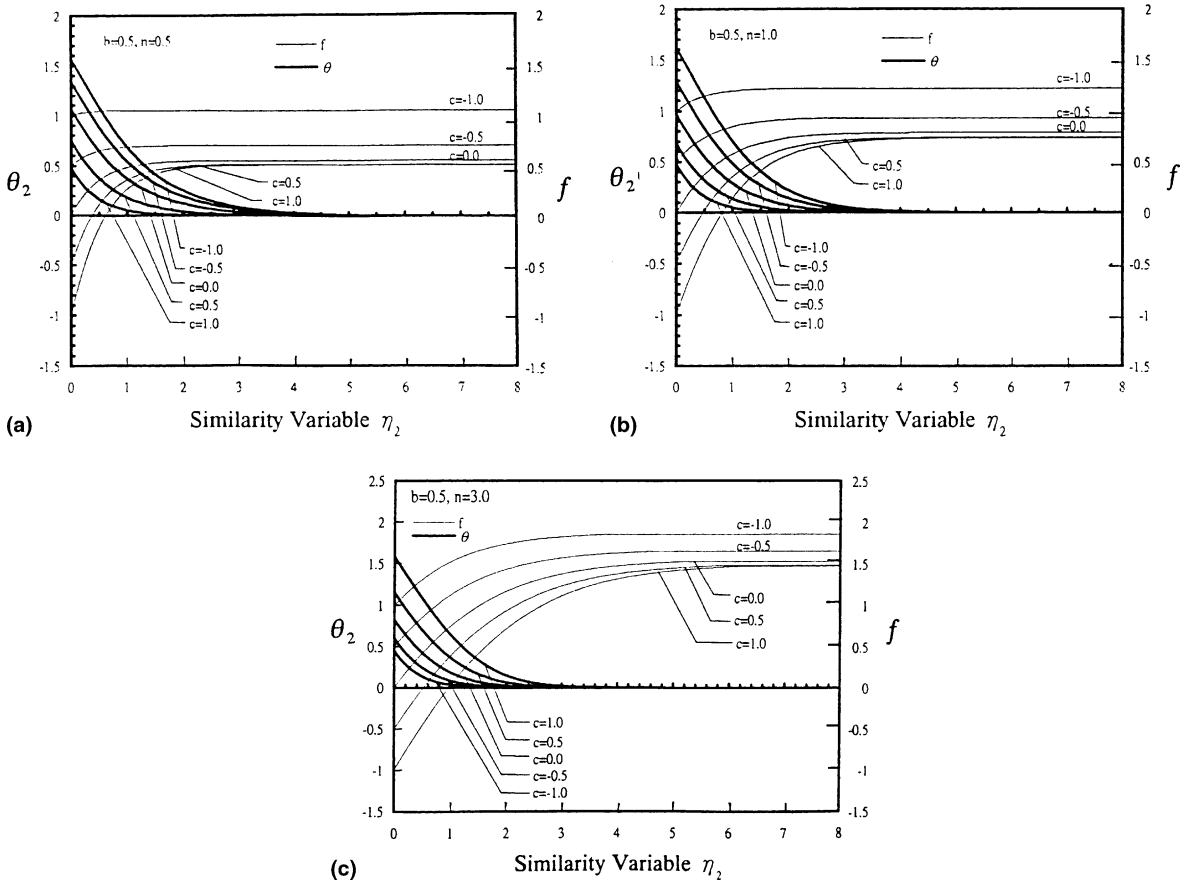

Fig. 12. The dimensionless temperature and similarity stream function profiles versus η_2 for various values of permeable constant c when $b = 0.5$, $n = 3.0$ in the condition 4.

$$q_w^*(x^*) = Ra_n^{1/2}(x^*)^b, \tag{85}$$

$$Nu_x = Ra_n^{1/2}(x^*)^{(b+n+1)/(2n+1)}a^{1/(2n+1)}/\theta_2(0), \tag{86}$$

$$\overline{h} = \frac{(2n+1)k_{ef}a^{1/(2n+1)}}{(b+n+1)\ell\theta_2(0)}Ra_n^{1/2}, \tag{87}$$

$$\overline{Nu} = \frac{(2n+1)a^{1/(2n+1)}}{(b+n+1)\theta_2(0)}Ra_n^{1/2}, \tag{88}$$

$$Q^* = 2\pi^m(W^*)^{(1-m)}Ra_n^{1/2}(1-a^2)^{1/2}/(b+m+1), \tag{89}$$

where $b > -(n+1)$ and $b > -(m+1)$. For a fixed value of n and value of c, the value of heat transfer rate $\overline{Nu}/Ra_n^{1/2}$ increases with increasing a; otherwise, the value of heat transfer rate $\overline{Nu}/Ra_n^{1/2}$ decreases as an increase in the value of c, for a fixed value of n and value of a, as in Fig. 13. Therefore, it is concluded that both increasing n and decreasing c have better effects on the heat transfer.

4. Conclusions

The local non-similarity method is applied in this theoretical study. The fourth-order Runge–Kutta

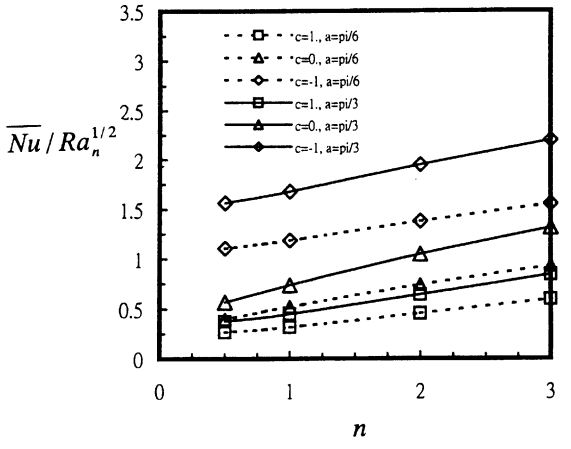

Fig. 13. The values of $\overline{Nu}/Ra_n^{1/2}$ versus power index n for various values of angle a and permeable constant c in the condition 4.

scheme method and shooting method are employed to analyze the steady-state natural convection external fluid flow and heat transfer over the permeable two-dimensional or three-dimensional axisymmetric bodies in a fluid-saturated porous medium filled with one of the non-Newtonian fluids. The governing boundary layer equations and boundary conditions are changed into a dimensionless form by the local non-similarity transformations and the resulting equations are solved by the method above. Let us take notice of the value of $\eta_\infty \leqslant 10.0$ for solving solutions usually in the past documents. In this study, particularly, we have to set enough large values $\eta_\infty \geqslant 20$ for the condition 1 in case 1 and $\eta_\infty \geqslant 30$ for the condition 3 in case 2. Otherwise, the numerical results will produce very large errors.

Commendably, the exact solutions are found in the conditions 2 and 4, respectively. From the numerical results obtained in this study, it showed that the beginning of natural convection would take place if certain inequality of the dimensionless yield stress is provided. The dimensionless thermal boundary layer thickness δ_t increases with decreasing the value of power index n and decreases as the value of the permeable constant c decreases. The predictions of dimensionless temperature θ and stream function f profiles are presented. The results are in good agreement with the exact solutions within 0.157% discrepancy. It is concluded that both increasing n and decreasing c have better effects on the heat transfer, when the value of a is fixed, namely, the geometry of body is fixed.

References

[1] P. Cheng, The influence of lateral mass flux on free convection boundary layers in a saturated porous medium, Int. J. Heat Mass Transfer 20 (1977) 201–206.

[2] J.H. Merkin, Free convection boundary layer in a saturated porous medium with lateral mass flux, Int. J. Heat Transfer 21 (1978) 1499–1504.

[3] C.Y. Liu, Note on free convection boundary layer in a saturated porous medium with lateral mass flux, Lett. Heat Mass Transfer 8 (1981) 167–169.

[4] J.H. Merkin, Free convection boundary layer on axisymmtric and two-dimensional bodies of arbitrary shape in a saturated porous medium, Int. J. Heat Transfer 22 (1979) 1461–1462.

[5] A. Nakayama, H. Koyama, Free convective heat transfer over a nonisothermal body of arbitrary shape embedded in a fluid-saturated porous medium, J. Heat Transfer ASME 109 (1987) 125–130.

[6] W.J. Minkowycz, P. Cheng, Local non-similar solutions for free convective flow with uniform lateral mass flux in a porous medium, Lett. Heat Mass Transfer 9 (1982) 159–168.

[7] A. Acrivos, A theoretical analysis of laminar natural convection heat transfer to non-Newtonian fluids, AIChE J. 6 (1960) 584–590.

[8] I.G. Reilly, C. Tien, M. Adelman, Experimental study of natural convective heat transfer from a vertical plate in a non-Newtonian fluid, Can. J. Chem. Eng. 8 (1965) 157–160.

[9] R.M. McKinley, H.O. Jahns, W.W. Harris, Non-Newtonian flow in porous media, AIChE J. 12 (1966) 17–24.

[10] H. Pascal, Rheological behaviour effect of non-Newtonian fluids on steady and unsteady flow through a porous media, Int. J. Numer. Anal. Meth. Geomechanics 7 (1983) 289–303.

[11] H. Pascal, Some problems related to the quantitative evaluation of physical properties of the porous medium from flow tests with non-Newtonian fluids, Int. J. Eng. Sci. 23 (1985) 307–317.

[12] H. Pascal, Flow of non-Newtonian fluid through porous media, Int. J. Eng. Sci. 23 (1985) 571–585.

[13] C.K. Chen, H.T. Chen, Natural convection of a non-Newtonian fluid about a horizontal cylinder and a sphere in a porous medium, Int. Commun. Heat Mass Transfer 15 (1988) 605–614.

[14] H. Pascal, F. Pascal, On viscoelastic effects in non-Newtonian steady flows through porous media, Transp. Porous Media 4 (1989) 17–35.

[15] Y.-T. Yang, S.-J. Wang, Free convection heat transfer of non-Newtonian fluids over axisymmetric and two-dimensional bodies of arbitrary shape embedded in a porous medium, Int. J. Heat Mass Transfer 39 (1996) 203–210.

[16] G. Getachew, W.J. Minkowycz, D. Poulikakos, Natural convection in a porous cavity saturated with a non-Newtonian fluid, J. Thermophys. Heat Transfer 10 (1996) 640–651.

[17] K.A. Yih, Uniform lateral mass flux effect on natural convection of non-Newtonian fluids over a cone in porous media, Int. Commun. Heat Mass Transfer 25 (1998) 959–968.

[18] C.Y. Cheng, An integral approach for heat and mass transfer by natural convection from truncated cones in porous media with variable wall temperature and concentration, Int. Commun. Heat Mass Transfer 27 (2000) 537–548.

[19] R.Y. Jumah, A.S. Mujumdar, Free convection heat and mass transfer of non-Newtonian power law fluids with yield stress from a vertical flat plate in saturated porous media, Int. Commun. Heat Mass Transfer 27 (2000) 485–494.

[20] R.B. Bird, W.E. Stewarnt, E.N. Lightfoot, in: Transport Phenomena, Wiley, Singapore, 1960, pp. 3–19.

[21] T. Al-Fariss, K.L. Pinder, Flow through porous media of a shear – thinning liquid with yield stress, Can. J. Chem. Eng. 65 (1987) 391–404.

[22] R.M. McKinley, H.O. Jahns, W.W. Harris, Non-Newtonian flow in porous media, AIChE J. 12 (1966) 17–24.